



Electronic properties of E3 electron trap in n-type ZnO

Gauthier Chicot, Julien Pernot, Jean-Louis Santailier, Céline Chevalier, Carole Granier, Pierre Ferret, Alexandre Ribeaud, Guy Feuillet, Pierre Muret

► To cite this version:

Gauthier Chicot, Julien Pernot, Jean-Louis Santailier, Céline Chevalier, Carole Granier, et al.. Electronic properties of E3 electron trap in n-type ZnO. *physica status solidi (b)*, 2014, 251 (1), pp.206-210. 10.1002/pssb.201349261 . hal-00936922

HAL Id: hal-00936922

<https://hal.science/hal-00936922>

Submitted on 30 Jan 2014

HAL is a multi-disciplinary open access archive for the deposit and dissemination of scientific research documents, whether they are published or not. The documents may come from teaching and research institutions in France or abroad, or from public or private research centers.

L'archive ouverte pluridisciplinaire **HAL**, est destinée au dépôt et à la diffusion de documents scientifiques de niveau recherche, publiés ou non, émanant des établissements d'enseignement et de recherche français ou étrangers, des laboratoires publics ou privés.

Electronic properties of E3 electron trap in *n*-type ZnO

G. Chicot,^{1,2, a)} J. Pernot,^{1,3} J. L. Santailier,² Céline Chevalier,² Carole Granier,² Pierre Ferret,² Alexandre Ribeaud,² G. Feuillet,² and P. Muret¹

¹⁾*Institut Néel, CNRS and Université Joseph Fourier, BP166,
38042 Grenoble Cedex 9, France*

²⁾*CEA-LETI, Minatec Campus, 17 rue des Martyrs, 38054 Grenoble Cedex 9,
France*

³⁾*Institut Universitaire de France, 103 boulevard Saint Michel, 75005 Paris,
France*

(Dated: 30 January 2014)

Deep level transient spectroscopy measurements were performed on three non-intentionally doped *n*-type ZnO samples grown by different techniques in order to investigate the electronic properties of E3 electron trap. The ionization energy and the capture cross section are found respectively at 0.275 eV from the conduction band and $2.3 \times 10^{-16} \text{ cm}^2$ with no electric field dependence. This center is present irrespective of the synthesis method. In view of its physical properties and recent works published in the literature, its physical origin is discussed. Based mainly on its insensibility to the macroscopic electric field, the best candidates turn out to be dual defects with opposite charges on adjacent sites, like the dual vacancy V_O - V_{Zn} .

^{a)}Electronic mail: gauthier.chicot@neel.cnrs.fr

I. INTRODUCTION

ZnO is a very attractive semiconductor for optoelectronic uses. Indeed, its wide direct band gap (3.37eV) and very large exciton binding energy (60meV), allow ZnO to compete with GaN for LED applications in the UV spectrum. However, p doping of ZnO is still a challenge due to intrinsic and extrinsic *n*-type conductivity. In this regards, the knowledge of deep levels is an important issue for optoelectronic devices elaboration. Firstly, assessing the presence of deep donors is useful both to understand the origin of *n*-type conduction and because *p*-type material will be obtained only if their effect is cancelled. Secondly, deep levels can act as non radiative centers that affect directly the light emission efficiency in p-n junction devices. Deep Level Transient Spectroscopy (DLTS) is a well adapted technique, as it can give physical properties of the deep levels such as their activation energy, capture cross section, trap concentration and their sensitivity to electric field.

In this work, we will focus on a deep level which is common to three non-intentionally doped *n*-type ZnO samples grown by three different techniques. This level is the well known E3 level, as quoted in literature, found very frequently in ZnO samples. However, its origin is still a matter of controversy¹⁻⁹.

This paper is organized as follows. In the second section, experimental details about samples and measurements are given. In the third section, DLTS results are analyzed in order to get very accurate values of the activation energy and capture cross section for the E3 level. Finally, physical origin of E3 is discussed in regards of the absence of electric field dependence of its signature and recent works published in literature.

II. EXPERIMENTAL DETAILS

In this work different kinds of sample were investigated : a MetalOrganic Vapor Phase Epitaxy (MOVPE) epilayer grown at CEA/LETI (label #1) on a commercial hydrothermal ZnO substrate (from Crystech Inc.), a crystal grown from the melt under high-pressure from Cermet Inc. (label #2) and a crystal grown by the hydrothermal method from Tokyo-Denpa Inc. (label #3). The MOVPE layer (#1) was grown at 950 °C using N₂O and DEZn as precursors. The epilayer is 525 nm thick as given by SIMS analysis. MOVPE layer was firstly cleaned with organic solvents and then processed with Remote Oxygen Plasma (ROP). The

sample grown from the melt at high-pressure (#2) was firstly annealed at 1100 °C in order to activate the shallow donors and receive the same conditioning as the hydrothermal sample, then treated by UV Ozone. The hydrothermally grown sample (#3) was firstly annealed at high temperature (1100 °C) by Tokyo-Denpa Inc., and then cleaned in organic solvents before being treated by ROP. On the three surfaces, Pt Schottky contacts (50 nm thick and 500 μm in diameter) were evaporated on the O face and full sheet Ti/Au ohmic contacts (20/80nm thick) were evaporated on the whole Zn face .

Capacitance voltage $C(V)$ and DLTS measurements were performed with a Phystech FT1030 that operates at 1MHz, a frequency which has been checked to be much less than the cut-off frequency of all the diodes. DLTS spectra were obtained from the fast Fourier transform (FFT) of the capacitive transients, delivering up to 23 Fourier coefficients. Current voltage ($I(V)$) measurements were firstly achieved to check the rectifying behavior of Pt contacts and the leakage current at different temperatures. $C(V)$ measurements were then performed at reverse bias voltage inducing low enough leakage currents to determine the effective doping profile $N_d - N_a$ (see figure 1). Finally DLTS analysis were performed from 80K to 500K with reverse bias (U_r) of -2 V, pulse voltage (U_p) of 0 V for sample #1 and #3 and with $U_r=-0.3$ V, $U_p=0.1$ V for sample #2 after a filling pulse of T_p duration. For all the three samples, different times windows (T_w) ranging between 10 ms and 500 ms were used in order to increase the number of points on the Arrhenius diagram.

III. RESULTS

DLTS spectra showed up several peaks, but only one (the E3 level) is common to the three samples described above. In figure 2, the experimental and simulated DLTS spectra found in the three samples are plotted. A good agreement appears between experimental and simulated spectra, the latter being calculated with a single emission time constant at each temperature (with parameters determined by the Arrhenius diagram, see below), generally associated to a point defect rather than to an extended defect for which fluctuating environment generates broadening of the emission rate distribution.

The Arrhenius diagram (figure 3) was obtained by extracting both temperature and emission rates from the maxima detected in DLTS spectra using up to 23 distinct and independent correlation functions yielding back as much Fourier coefficients¹⁰. By linear

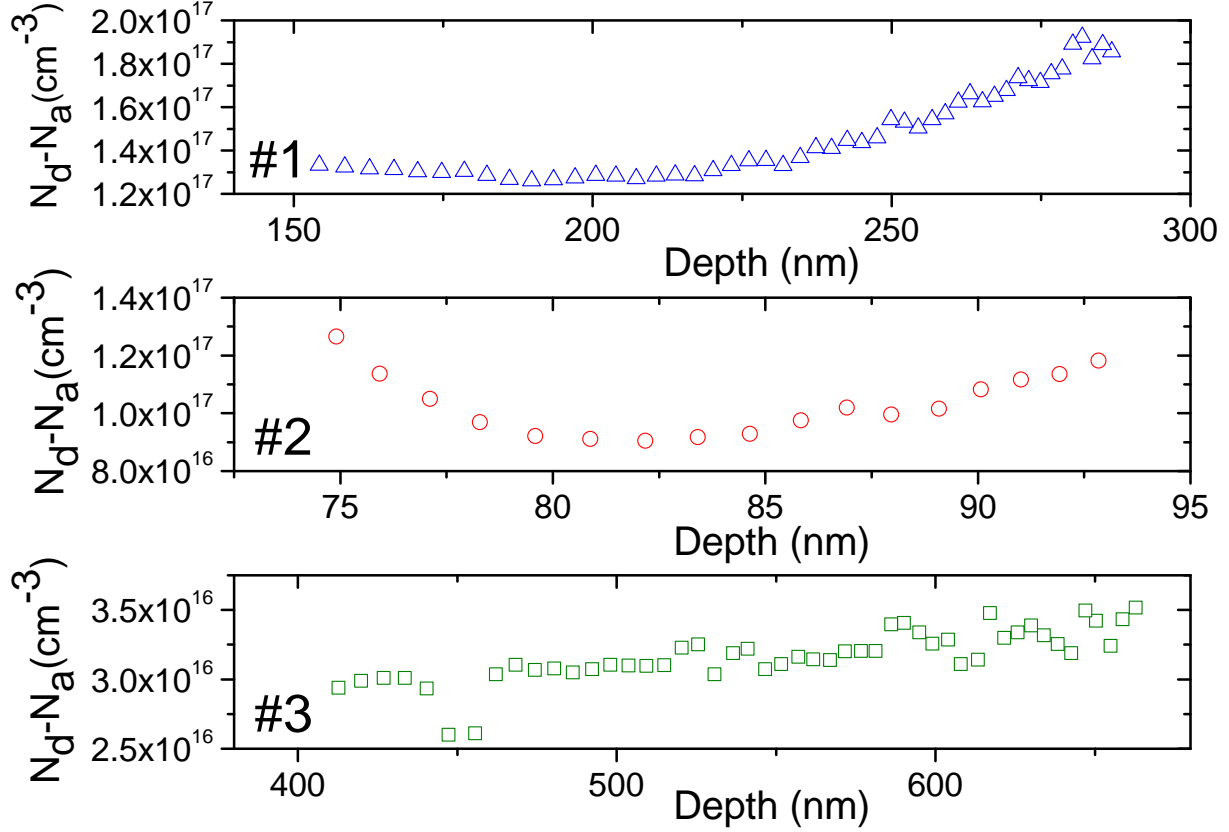


FIG. 1. $N_d - N_a$ versus depth obtained by C(V) measurement on (#1) MOVPE sample, (#2) high-pressure grown sample and (#3) hydrothermal sample.

fitting, the activation energy (from the slope) and the capture cross section (from the Y-intercept) can be obtained using the emission rate formula :

$$e_n = \sigma_n v_{th} N_C \exp\left(\frac{-E_{an}}{k_b T}\right) \quad (1)$$

where e_n is the emission rate, σ_n the apparent capture cross section, v_{th} the thermal velocity, N_C the effective density of states in the conduction band, E_{an} the activation energy, k_b the Boltzmann constant and T the temperature. The concentration of traps (deduced from the amplitude of the DLTS peaks and $N_d - N_a$) as well as the effective doping ($N_d - N_a$) and the mean value of the electric field experienced by the electron during the emission phase are reported in table I.

As one can see in Fig. 3, it is not possible to distinguish straight lines for each sample in the Arrhenius diagram showing that the origin of the traps is the same. Several consequences come from this evidence. Firstly, global values for the activation energy and capture

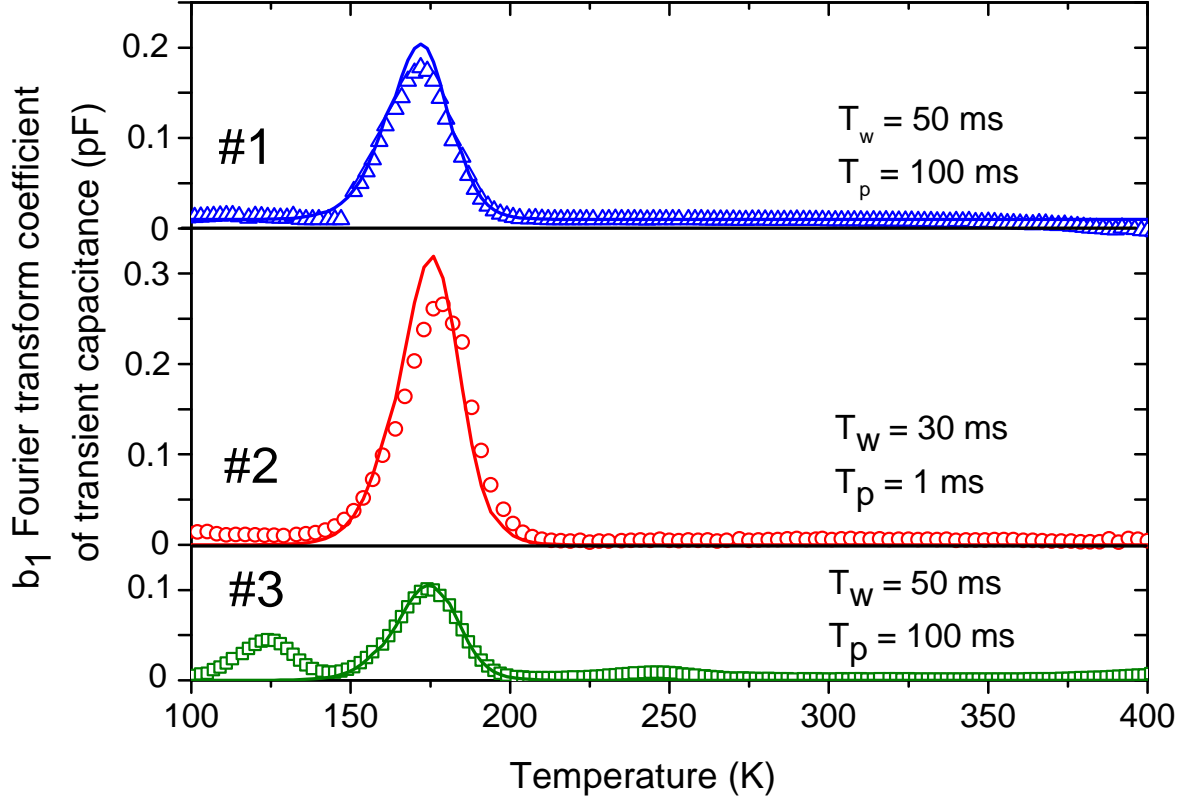


FIG. 2. Experimental and simulated DLTS signal for (#1) MOVPE sample, (#2) high-pressure grown sample and (#3) hydrothermal sample. The lines are the simulated signal for the E3 level for each sample.

TABLE I. Properties of the three *n*-type ZnO samples : average density of the E3 level (N_T), average effective doping level ($\langle N_d - N_a \rangle$), and mean value of the electric field (F) experienced by the electron during the emission phase (see Eq. 4).

Samples	N_T (cm ⁻³)	$\langle N_d - N_a \rangle$ (cm ⁻³)	$ F $ (MV.cm ⁻¹)
#1	$8.0 \times 10^{+15}$	$1.5 \times 10^{+17}$	0.19
#2	$1.5 \times 10^{+15}$	$1.0 \times 10^{+17}$	0.09
#3	$8.6 \times 10^{+14}$	$3.1 \times 10^{+16}$	0.07

cross section can be obtained from an overall least mean square fit (line in figure 3) of all the $(T; e_n)$ points : $E_a = 0.275 \pm 0.002$ eV and $\sigma_n = 2.3 \pm 0.3 \times 10^{-16}$ cm² where the uncertainties are derived from the standard deviations and ensure that the actual values lie within this confidence interval with a 95 per cent probability. The fairly small capture cross section is characteristic of a neutral or eventually repulsive trap before electron capture, confirming the Auret et al.⁵ observation.

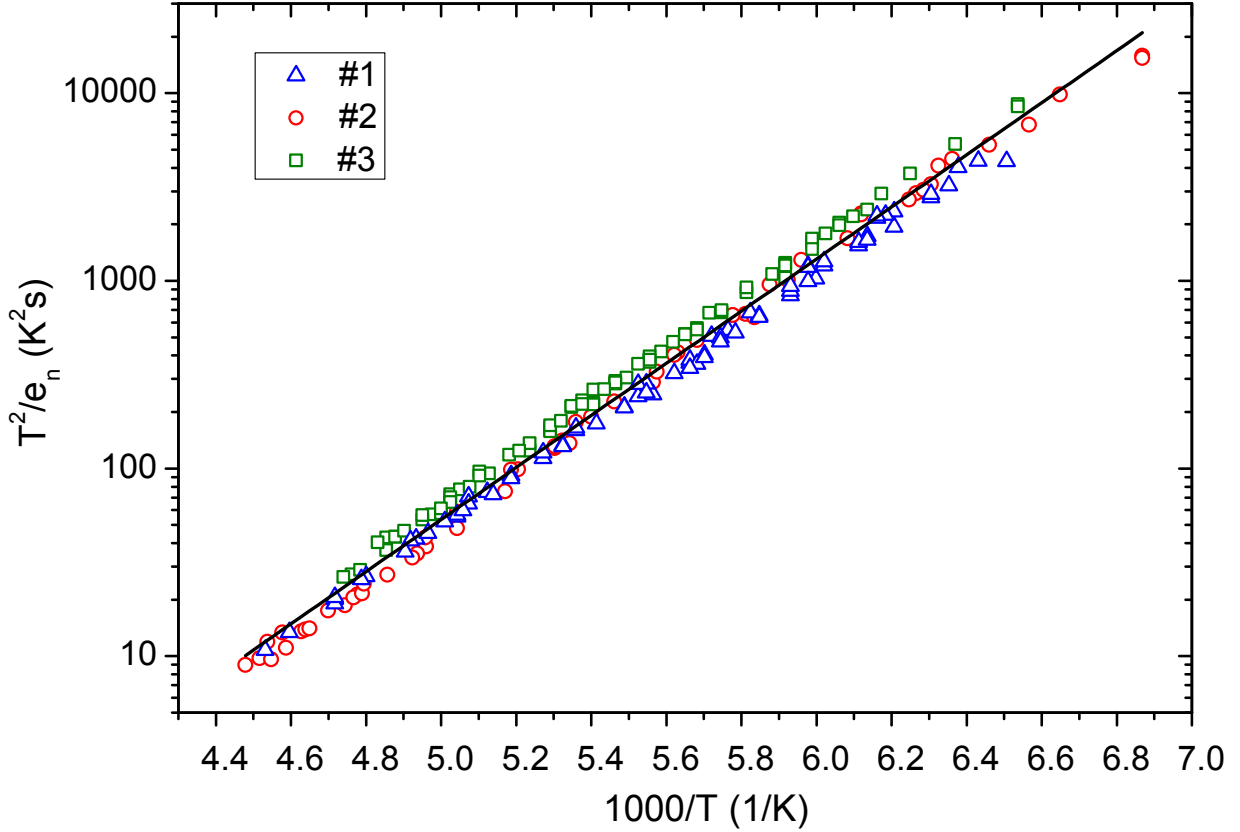


FIG. 3. Arrhenius diagram of E3 level for #1 MOVPE layer (open triangle), #2 high-pressure grown samples (open circle) and #3 hydrothermally grown sample (open square). The solid line is the global fit of all these points.

The sample diversity in term of doping level (cf. table I) enable us to investigate the effect of electric field. The electric field versus depth $F(x)$ was calculated using the integrated Poisson equation :

$$F(x) = \frac{e \langle N_d - N_a \rangle}{\epsilon_r \epsilon_0} (x - w(U_r)) \quad (2)$$

where e is the elementary charge, $\langle N_d - N_a \rangle$ the average effective doping given in table I,

$\epsilon_r = 8$ the relative permittivity of ZnO, ϵ_0 the vacuum permittivity, $w(U_r)$ the WSCR under U_r bias obtained by $w(U_r) = \epsilon_r \epsilon_0 S / C(U_r)$ (S is the Schottky contact area), and x the abscissa along the WSCR which origin is at the Schottky contact/semiconductor interface. As N_T is negligible compared to $< N_d - N_a >$, the abscissa where the quasi-Fermi level E_F coincides with the energy level of the trap E_T ¹¹ is defined by $w(V) - L_0$ (where V is the applied voltage) where

$$L_0 = L_D \sqrt{2} \left(\frac{E_F - E_T}{k_b T} - 1 \right)^{1/2} \quad (3)$$

with L_D the Debye length. Considering a full filling of the traps, the electrons released during the emission phase come from the range of abscissa between $w(U_p) - L_0$ and $w(U_r) - L_0$. The mean value of electric field experienced by an electron captured under U_p bias and released under U_r bias (given in table I) is calculated using the formula 2 as follow :

$$F = \frac{F(w(U_p) - L_0) + F(w(U_r) - L_0)}{2} \quad (4)$$

The electric field can affect the emission rate along different mechanisms¹²⁻¹⁶ : Poole-Frankel effect, phonon assisted tunneling effect or direct tunneling effect. Considering only the Poole-Frankel effect for a Coulombic potential using the model described in Ref.¹³, we should find a emission rate more than 10 times greater for sample #1 than for sample #3, that is obviously not the case on the Arrhenius diagram (Fig. 3). Thus, no significant dependence of the electric field on the emission rate is observed (also noticed by Auret et al.⁵) in agreement with a neutral trap before electron capture. This observation is valid for mean electric field values varying from 0.07 MV.cm⁻¹ to 0.19 MV.cm⁻¹. In sample #1 (i.e. highest doping level), experiments with higher reverse voltage U_r were performed in order to widen the electric field range of investigation of this work. Unfortunately, the deeper space charge region (region probed by DLTS) includes an additional deep level with an emission time constant very close to the one of the E3 level, which makes the interpretation of the Arrhenius diagrams unreliable at such reverse voltage.

Therefore, it appears that the E3 level is a very deep acceptor, lying 0.275 eV below the conduction band, since it becomes negatively charged after electron capture and hence experiences a 0/- elementary charge change.

IV. DISCUSSION

By finding the E3 level in three different samples, we confirm its presence, irrespective of the synthesis method used to grow the samples considered here. In other studies, this level has also been detected in vapor phase grown samples^{1,3,5,8}, in PLD thin films^{6,7} and in hydrothermally grown sample⁴. Therefore, E3 is a defect found in both single crystal and polycrystalline ZnO, that had been formerly attributed to isolated oxygen vacancies $V_O^{1,2,8}$. But this assumption is now under debate : recently von Wenckstern et al.⁶ found that the concentration of E3 in annealed samples is independent of the annealing ambient. Monakhov et al.² also questioned this attribution because the peak associated to E3 has a very weak dependence on the ions irradiation dose and, thus, an assignment to a primary defect as V_O is not obvious. Other observations, along the same way, show that the Schottky pre-treatments (such as oxygen plasma, H_2O_2 treatment, UV ozone) which are supposed to bring in oxygen atoms have no effect on E3². These experimental facts are in agreement with theoretical calculations from Janotti et al.¹⁷. Indeed, ab initio calculations based on Local Density Approximation show that the singly charged oxygen vacancy V_O^+ cannot be stable because of too a high formation energy. Only V_O^{2+} is stable in ZnO and its activation energy for the transition (2+,0) is estimated to be 1 eV or more.

Profiling using DLTS isothermal measurements was performed on the sample #1 (MOVPE layer). The E3 trap concentration increases with depth away from the surface, when the interface with the substrate is approached. In the case of the MOVPE epilayer, if E3 were attributed to V_O , the increasing concentration with depth could be due to the effect of the ROP filling the oxygen vacancies more efficiently near the surface than deeper into the layer. But considering that E3 probably experiences (0/-) charge states in contrast to (2+,0) for V_O , with an energy around 1.2 eV for the transition¹⁷, an assignment of E3 to the donor V_O is highly unlikely. However, a complex involving an oxygen vacancy cannot be discarded.

Since the E3 level appears in ZnO whatever the fabrication technique, this level is related to a native defect (such as a vacancy, for example) or to an impurity which is always present in ZnO. Therefore two hypothesis can be formulated :

i) On the one hand E3 might be assigned to an impurity. DLTS and SIMS analysis were led on a total of 10 samples (4 grown by Chemical Vapor Transport, 4 by hydrothermal

method, 1 by high pressure melt method and 1 by MOVPE). E3 level was detected in 5 of these samples but no clear correlation between E3 presence and impurities (Li, Fe, Al, N, C, Si) concentration was found. It must be noticed that the SIMS detection limit of such impurities is in most cases larger than N_T detected by DLTS. So, an attribution to an impurity cannot be discarded.

ii) On the other hand, as the level is present whatever the growth method, an attribution to a native defect seems also to be more relevant. Assignment of E3 to the isolated V_O has been previously discarded but a complex involving V_O may be considered. An attribution of E3 to the isolated V_{Zn} is also not possible since V_{Zn} is too deep (2.1 eV below the conduction band) to be detected by DLTS⁹. Recently, Dong et al.⁹ proposed that the E3 might be related to a complex involving V_O such as V_O - V_{Zn} . Although based on other statements that those contained in Dong et al. paper⁹, the origin of E3 may rely on a complex involving two defects or impurities charged differently on adjacent sites, due to the insensibility of E3 physical properties to the electric field that we have demonstrated in this work. Such a combination of the two previous cases is discussed deeper in the following.

All the models, either semi-classical^{12,13} or involving quantum theory¹⁴⁻¹⁶, dealing with the influence of the electric field on the deep level of an isolated charged impurity, concluded to a strong effect, typically of several hundreds of percents for the variation of the emission rate when the field varies only of some tens of percents. No such effect were observed on our sample even considering only Poole-Frenkel effect. All these models assume that the deep level lies in a potential well of spherical symmetry around the impurity, which originates from the charge including the nucleus and the inner electrons located on the rare gas core of the foreign atom, thus producing a net positive charge. Adding the valence electrons cloud may change the net global charge of the potential well felt by itinerant carriers. But in any case, such a picture led invariably to a deformation of the potential well by the macroscopic electric field and therefore to strong changes of the emission rate¹⁸, contrary to what happens for the E3 level. Consequently, the E3 level cannot be related to an isolated impurity alone, either substitutional or interstitial. On the contrary, if either the positively charged center is missing, like in the vacancy case, or a two centers defect is present with different charges on the two adjacent sites, the insensibility of the E3 level to the macroscopic electric field can be understood because the former is so weaker than the internal field inside this defect (about $10^{10} V m^{-1}$ for two elementary charges with opposite signs on two adjacent sites) that

its effect is negligible. In other words, the shape of the potential well of such a defect is so asymmetric that it cannot be appreciably changed by the macroscopic field. Because isolated V_O or V_{Zn} are not likely, dual center defects with different charges and probably opposite ones on each site to give a net neutral center are the best candidates. Hence, the E3 level could be due to either the dual vacancy V_O - V_{Zn} , or the combination of an interstitial and a substitutional impurity like Li_{Zn} - Li_i or any impurity associated to a vacancy, provided their charges are opposite.

V. CONCLUSION

DLTS measurements performed on three samples provided accurate values of activation energy and capture cross section for the well known E3 electron trap. DLTS technique and associated characterization methods also provided interesting characteristics about E3 such as its presence whatever the synthesis method used for the fabrication of the sample, its independence to electric field and the prominence of this peak in all three samples. Neither an attribution to a native defect (like V_O) nor to an impurity can be firmly established but a dual center defect composed of two sites with opposite charges is very probable.

The authors gratefully acknowledge support from National Research Agency (ANR) and Carnot funding.

REFERENCES

- ¹F. D. Auret, S. A. Goodman, M. J. Legodi, W. E. Meyer, and D. C. Look, Appl. Phys. Lett. **80**, 1340 (2002).
- ²E. V. Monakhov, A. Y. Kuznetsov, and B. G. Svensson, J. of Phys. D: Appl.Phys. **42**, 153001 (2009).
- ³Z. Q. Fang, B. Claffin, D. C. Look, Y. F. Dong, and L. Brillson, J. Vac. Sci. Technol. B **27**, 1774 (2009).
- ⁴H. von Wenckstern, H. Schmidt, M. Grundmann, M. W. Allen, P. Miller, R. J. Reeves, and S. M. Durbin, Appl. Phys. Lett. **91**, 022913 (2007).
- ⁵F. D. Auret, S. A. Goodman, M. Hayes, M. J. Legodi, H. A. van Laarhoven, and D. C. Look, J. Phys. : Cond. Mat. **13**, 8989 (2001).

- ⁶H. von Wenckstern, G. Biehne, M. Lorenz, M. Grundmann, F. D. Auret, W. E. Meyer, M. Hayes, and J. M. Nel, J. Korean Phys. Soc. **53**, 2861 (2008).
- ⁷F. D. Auret, W. Meyer, P. J. van Rensburg, M. Hayes, J. Nel, H. von Wenckstern, H. Schmidt, G. Biehne, H. Hochmuth, M. Lorenz, and M. Grundmann, Physica B: Cond. Mat. **401-402**, 378 (2007).
- ⁸Z. Q. Fang, B. Claflin, D. C. Look, Y. F. Dong, H. L. Mosbacker, and L. J. Brillson, J. Appl. Phys. **104**, 063707 (2008).
- ⁹Y. Dong, Z. Q. Fang, D. C. Look, D. R. Doutt, G. Cantwell, J. Zhang, J. J. Song, and L. J. Brillson, J. Appl. Phys. **108**, 103718 (2010).
- ¹⁰S. Weiss and R. Kassing, Solid-State Electronics **31**, 1733 (1988).
- ¹¹D. Pons, J. Appl. Phys. **55**, 3644 (1984).
- ¹²G. Vincent, A. Chantre, D. Bois, J. Appl. Phys. **50**, 5484 (1979).
- ¹³P. Martin, B. Streetman, K. Hess, J. Appl. Phys. **52**, 7409 (1981).
- ¹⁴S. Makram-Ebeid, M. Lannoo, Phys. Rev. Lett. **48**, 1281 (1982).
- ¹⁵S. Makram-Ebeid, M. Lannoo, Phys. Rev. B **25**, 6406 (1982).
- ¹⁶E. Korol, Soviet. Phys. Solid State **19**, 1327 (1977).
- ¹⁷A. Janotti and C. G. V. de Walle, Appl. Phys. Lett **87**, 122102 (2005).
- ¹⁸S. Ganichev, E. Ziemann, W. Prettl, I. Yassievich, A. Istratov, E. Weber, Phys. Rev. B **61**, 10361 (2000).